XIII International Conference on Computational Plasticity. Fundamentals and Applications
COMPLAS XIII
E. Oñate, D.R.J. Owen, D. Peric & M. Chiumenti (Eds)

ATOMISTIC MODELING AND SIMULATION OF LONG-TERM TRANSPORT PHENOMENA IN NANOMATERIALS

M.P. ARIZA*, C.S. MARTIN* AND M. ORTIZ†

* Escuela Técnica Superior de Ingeniería
Universidad de Sevilla
Camino de los descubrimientos, s.n. 41092-Sevilla, Spain
e-mail: mpariza@us.es, csmartin@us.es, web page: http://personal.us.es/mpariza/

†Engineering and Applied Sciences Division
California Institute of Technology
1200 E. California Blvd. Pasadena, 91125 CA, USA
e-mail: ortiz@caltech.edu, web page: http://aero.caltech.edu/ ortiz/index.html

Key words: Meanfield theory, non-equilibrium statistical thermodynamics, slow kinetic processes, thermal conductivity, semiconductor nanowire

Abstract. In the past two decades, extensive research has been conducted towards developing nanomaterials with superior transport properties, such as heat conductivity and mass diffusivity, for applications in various industries including, but not limited to, energy storage and microelectronics. In terms of modeling and simulation, a long-standing difficulty lies in the separation of temporal and spatial scales. Indeed, many transport phenomena in nanomaterials are characterized by slow kinetic processes with time scale of the order of seconds, hours, or even years, far beyond the time windows of existing simulation technologies such as molecular dynamics (MD) and Monte Carlo (MC) methods. We have developed a novel deformation-diffusion coupled computational framework that allows long-term simulation of such slow processes, while at the same time maintains a strictly atomistic description of the material. Our non-equilibrium statistical thermodynamics model includes discrete kinetic laws, which govern mass diffusion and heat conduction at atomic scale. In this work, we explore the capabilities and performance of this computational framework through its application to heat conduction problems.

1 INTRODUCTION

The thermal conductivity of a material (κ) is an intrinsic property which relates its ability to conduct heat. A highly thermally conductive material might be used as a heat exchanger cooling system, commonly required to improve the performance of high-power

semiconductor devices. Whereas materials of low κ are used as insulators when thermal conduction or thermal radiation needs to be reduced or reflected rather than absorbed, respectively. This later group of materials are recently intended for energy efficient applications, in which the performance of thermoelectric energy conversion devices depends on the thermoelectric figure of merit (ZT) of the material [1].

Many silicon-based materials have been extensively used for electronic applications. Although the semiconductor characteristics of pure silicon are not noticeable, silicon compounds and its alloys have been widely used as semiconductor devices. Among others, Silicon Carbide (SiC) was one of the first semiconductor materials that captured the attention of the electronics industry due to its excellent performance at high temperature [2], together with high power capabilities. Its wide bandgap (five times wider at room temperature than the one corresponding to Si) and high durability, electrical breakdown field and thermal conductivity, led to focus much attention to the development of growth techniques for the improvement of this silicon compound. Within the range of high power electronic devices, high values of κ is a desirable attribute, although this is not always the case.

The development of renewable energy technologies has created the need for novel materials with high efficient thermoelectric behavior, that is defined in terms of their ZT, which is inversely proportional to κ. The value of this parameter has been reported [3, 1] to be enhanced beyond unity by nanostructuring thermoelectric materials, mostly due to the reduction of the thermal conductivity when the representative section is reduced below the electron and/or phonon mean free path [4]. Although bulk silicon is a poor thermoelectric material, silicon based nanostructures in the form of one-dimensional conductors or nanowires have been investigated as potentially efficient thermoelectric materials for more than twenty years [5]. Silicon nanowires (SiNW) have been proposed to be a crucial component for the manufacturing of nanoelectronic devices, therefore their synthesization process [6, 7] and measuring of thermal and electrical properties have challenged many researchers in the past decade [8, 9, 10, 11].

It was well established that thermal conductivity of materials is temperature dependent, however the rise in the manufacturing of nanosize electronic components has highlighted that κ relies heavily on the size. Moreover, thermal properties of SiNWs have revealed to be strongly dependent on surface morphology [6].

Much computational effort have been devoted to comprehend heat transport in very thin SiNW. [12] have computed the heat conductance for ultrathin SiNWs (diameters ranging from 1 to 5 nm) using density functional theory and Tersoff empirical potential for thicker sections, showed that thermal behavior is heavily anisotropic. They have found that wire orientation influences the ballistic thermal conductance of SiNWs about 50% to 75%. More recently, atomistic simulations carried out by [13] have confirmed that the existence of a disordered surface as thin as two atomic layers is sufficient to reduce κ by an order of magnitude with respect to that of crystalline wires with the same radius.

The first measurement of the thermal conductivity of SiNWs was reported by [8]. They

obtained thermal conductivities for individual nanowires with diameters ranging from 22 to 115 nm more than two orders of magnitude lower than the bulk value. More recent works by [10] and [11] have reasserted the pioneering results for VLS-grown wires with relatively smooth surfaces, and extended their study by focusing on the phonon-boundary scattering for thinner nanowires.

Here, we specifically aim to ascertain the ability of models based on non-equilibrium statistical mechanics, specifically, the approach proposed by Kulkarni et al. [14] and Venturini et al. [15], to reproduce the observed anisotropy, temperature and size dependence of the thermal conductivity of silicon nanowires.

2 COMPUTATIONAL MODEL

In this numerical study, we show that this significant size effect can be reproduced using the discrete linear Fourier law proposed above. Following the experimental study of [8], we consider single crystal Si nanowires oriented in the $\langle 111 \rangle$ direction, with diameters $D = 22,\ 37,\ 58,$ and 115 nm. We assume the Si atoms in the nanowires are fixed" in a meanfield sense, that is, the mean atomic position $\{\overline{\boldsymbol{q}}\}$ is constant in time, and the mean atomic momentum $\{\overline{\boldsymbol{p}}\}$ is zero. This assumption can be justified because in the experiment, temperature variation is small (less than 5 K). Moreover, we assume the particle temperature θ at each atom is also constant in time, which can be justified because all the experimental measurements are conducted at steady state [9].

At about 3 μm long, the nanowires used in the experiment contain 30 million to 1 billion atoms. Therefore, simulating the entire nanowire in an atomistic description is prohibitively expensive. To circumvent this difficulty, we recourse to the homogenization theory for an inhomogeneous rigid conductor, and mirror it to the atomistic samples.

We first consider an inhomogeneous rigid conductor occupying $\Omega \in \mathcal{R}^3$ with prescribed average temperature derivative along x_i-axis, denoted by $\overline{T}_{,i}$. Assuming heat conduction is governed by the linear Fourier law, the temperature field T is the solution of

$$(\kappa_{ij}(\boldsymbol{x})T_{,j})_{,i} = 0, \qquad \text{in } \Omega, \tag{1a}$$

$$\frac{1}{|\Omega|}\int_\Omega T_{,i}d\boldsymbol{x} = \overline{T}_{,i}, \qquad \text{on } \partial\Omega, \tag{1b}$$

which can be written in variational form as

$$\min_T \int_\Omega \frac{1}{2}\kappa_{ij}(\boldsymbol{x})T_{,i}T_{,j}d\boldsymbol{x}, \tag{2a}$$

$$\text{s.t. } \frac{1}{|\Omega|}\int_\Omega T_{,i}d\boldsymbol{x} = \overline{T}_{,i}, \tag{2b}$$

or equivalently,

$$\min_{T} \int_{\Omega} \frac{1}{2}\kappa_{ij}(\boldsymbol{x})T_{,i}T_{,j}d\boldsymbol{x}, \tag{3a}$$

$$\text{s.t. } \frac{1}{|\Omega|}\int_{\partial\Omega} T\boldsymbol{n}_i \cdot d\boldsymbol{\sigma} = \overline{T}_{,i}, \tag{3b}$$

With Lagrange multiplier $\overline{J}_i$, (3) can be re-written as

$$\min_{T,\overline{J}_i} \int_{\Omega} \frac{1}{2}\kappa_{ij}(\boldsymbol{x})T_{,i}T_{,j}d\boldsymbol{x} - \overline{J}_i\big(\frac{1}{|\Omega|}\int_{\Omega} T_{,i}d\boldsymbol{x} - \overline{T}_{,i}\big), \tag{4}$$

leading to the following equilibrium conditions:

$$(\kappa_{ij}(\boldsymbol{x})T_{,j})_{,i} = 0, \qquad \text{in } \Omega, \tag{5a}$$

$$J_i\boldsymbol{n}_i = (\kappa_{ij}(\boldsymbol{x})T_{,j})\boldsymbol{n}_i = \overline{J}_i\boldsymbol{n}_i, \qquad \text{in } \Omega, \tag{5b}$$

$$\frac{1}{|\Omega|}\int_{\Omega} T_{,i}d\boldsymbol{x} = \overline{T}_{,i}, \qquad \text{on } \partial\Omega. \tag{5c}$$

From the second equation, we obtain

$$\frac{1}{|\Omega|}\int_{\partial\Omega} J_j n_j x_i d\sigma = \frac{1}{|\Omega|}\int_{\partial\Omega} \overline{J}_i n_j x_i d\sigma = \overline{J}_j \frac{1}{|\Omega|}\int_{\partial\Omega} n_j x_i d\sigma = \overline{J}_j\delta_{ij} = \overline{J}_i. \tag{6}$$

By linearity, there is a linear relation between the average flux $\overline{J}_i$ and the average temperature gradient $\overline{T}_{,i}$, namely,

$$\overline{J}_i = \overline{\kappa}_{ij}\overline{T}_{,i}, \tag{7}$$

which identifies the effective conductivities $\overline{\kappa}_{ij}$.

Now we mirror the above framework to the atomistic description of the Si nanowires. For each nanowire, we identify Ω as a slice of it containing 20 (111) planes of atoms. We set up a Cartesian coordinate system such that its z coordinate coincides with the axis of the nanowire. We fix the temperature of one atom to the ambient temperature at which heat conduction takes place (denoted by T_0), and set the average temperature gradient $\overline{T}_{,z}$ by

$$\overline{T}_{,z} = \frac{\Delta T}{L}, \tag{8}$$

where $\Delta T = 5.0$ K is (roughly) the maximum temperature variation observed in the experiment, and $L = 3.0 \times 10^3$ nm is (roughly) the length of the nanowires.

Then, $\{\theta\}$ and $\overline{J}_z$ are determined by

$$\min_{\{\theta\},\overline{J}_z,\mu} \sum_{i,j\in\Omega, i\neq j} \frac{1}{2}A_{ij}\theta_{ij}^2 P_{ij}^2 - \frac{\overline{J}_z}{\overline{T}_0^2}\Big(\sum_{i\in\partial\Omega}\theta_i(\boldsymbol{n}_i\cdot\boldsymbol{n}_z)\sigma_i - |\Omega|\overline{T}_{,z}\Big) - \mu(\theta_{i_0} - T_0) \tag{9}$$

with

$$\theta_{ij} = \frac{\theta_i + \theta_j}{2}, \tag{10}$$

and

$$P_{ij} = \frac{1}{\theta_i} - \frac{1}{\theta_j}. \tag{11}$$

Here, $\partial\Omega = \Gamma_f \bigcup \Gamma_l$ includes the first and last (111) planes of the nanowire slice, denoted by Γ_f and Γ_l, respectively. σ_i is the cross-sectional area of the nanowire associated with atom $i \in \partial\Omega$, determined in the present work by

$$\sigma_i = \frac{\pi R^2}{N_S}, \tag{12}$$

where N_S denotes the total number of atoms on each (111) plane. $\boldsymbol{n}_i$ and $\boldsymbol{n}_z$ denote the unit outward normal of $\partial\Omega$ at atom $i \in \partial\Omega$ and the direction of z-axis, respectively.

Enforcing stationarity of the objective function in Eq. 9 yields the following equilibrium conditions:

$$\sum_{j\in\Omega, j\neq i} A_{ij}\frac{\theta_i^4 - \theta_j^4}{4\theta_i^3\theta_j^2} + \frac{\overline{J}_z\sigma_i}{\overline{T}_0^2}\Big|_{i\in\Gamma_f} - \frac{\overline{J}_z\sigma_i}{\overline{T}_0^2}\Big|_{i\in\Gamma_l} - \mu\big|_{i=i_0} = 0, \qquad \forall i \in \Omega, \tag{13a}$$

$$\sum_{i\in\Gamma_l}\theta_i\sigma_i - \sum_{i\in\Gamma_f}\theta_i\sigma_i - |\Omega|\overline{T}_{,z} = 0, \tag{13b}$$

$$\theta_{i_0} - T_0 = 0. \tag{13c}$$

In this work, we solve Eq. (13) for $\{\theta\}$, $\overline{J}_z$, and μ using the Newton-Raphson method, and determine the effective thermal conductivity $\overline{\kappa}$ by

$$\overline{\kappa} = \frac{\overline{J}_z}{\overline{T}_{,z}}. \tag{14}$$

3 SIMULATION SETUP

The nanowires studied in the experiment carried out by [8] comprise an amorphous surface layer with thickness around 2 nm (see Fig. 2 of the aforementioned paper). We consider silicon nanowires with constant diameter which circular cross section consists of a crystalline core and an amorphous shell. However, due to the discreteness character of the silicon $\langle 111\rangle$ layers and the random distribution of atoms within the amorphous shell, a relatively small surface roughness is unavoidably introduced in our computational cell although the effect of phonon surface scattering on the thermal conductivity is out of the scope of this study. In particular, we account for the amorphous surface layer in our computational model by perturbing the positions of atoms located near the nanowire surface. More specifically, the mean atomic positions $\{\overline{\boldsymbol{q}}\}$ are determined by

$$\overline{\boldsymbol{q}}_i = \begin{cases} \overline{\boldsymbol{q}}_i^{(0)} + p_i\boldsymbol{d}_i, & \text{if i} \in \Omega_{\text{a}}; \\ \overline{\boldsymbol{q}}_i^{(0)}, & \text{otherwise}, \end{cases} \tag{15}$$

where $\overline{\boldsymbol{q}}_i^{(0)} = [q_{ix}^{(0)}, q_{iy}^{(0)}, q_{iz}^{(0)}]^T$ denotes the mean position of atom i in the perfect Si lattice with lattice constant $a = 0.543$ nm, and

$$\Omega_a = \left\{ \mathrm{i} \in \Omega \;\middle|\; \sqrt{\mathrm{q}_{\mathrm{ix}}^{(0)^2} + \mathrm{q}_{\mathrm{iy}}^{(0)^2}} > \mathrm{R} - \tau_{\mathrm{a}} \right\} \tag{16}$$

identifies atoms located within the amorphous surface layer. In order to build realistic crystalline/amorphous core/shell nanowires [16, 17], we have considered an amorphous shell with linearly varying thickness with the external diameter of the nanowire.

The thickness of the amorphous layer, denoted by τ_a in Eq. 16, is set to be 2 nm in all simulations. $\boldsymbol{d}_i$ and p_i are the randomly generated direction and magnitude of the perturbation applied to atom i. In this work, we draw $\boldsymbol{d}_i$ from the uniform distribution in unit sphere $S^2 = \{\boldsymbol{x} \in R^3 \mid \|\boldsymbol{x}\|_2 = 1\}$, and p_i from Gaussian distribution $N(\frac{p_{max}}{2}, (\frac{p_{max}}{8})^2)$, with $p_{max} = a/10$.

The discrete linear Fourier law used in Eqs. 9–13 allows heat conduction between each pair of atoms in Ω; and the bondwise conductivity coefficient A_{ij} can be different for each $\langle i, j \rangle$ pair. However, in order to achieve a computationally manageable model, here we restrict heat conduction within a small neighborhood, and assume A_{ij} can take only two values. More specifically, for all $i, j \in \Omega,\ i \neq j$, A_{ij} is determined by

$$A_{ij} = \begin{cases} A_a, & \text{if } i \in \Omega_a \text{ or } j \in \Omega_a,\ \|\overline{\boldsymbol{q}}_i - \overline{\boldsymbol{q}}_j\| < r_c; \\ A_c, & \text{if } i, j \in \Omega \setminus \Omega_a,\ \|\overline{\boldsymbol{q}}_i - \overline{\boldsymbol{q}}_j\| < r_c; \\ 0, & \text{if } \|\overline{\boldsymbol{q}}_i - \overline{\boldsymbol{q}}_j\| \geq r_c. \end{cases} \tag{17}$$

The cut-off radius r_c is chosen to be

$$r_c = \frac{a_1 + a_2}{2}, \tag{18}$$

where $a_1 = \frac{\sqrt{3}}{4}a$ and $a_2 = \frac{\sqrt{2}}{2}a$ are the distances between the first and second shells of closest neighbors in the perfect Si lattice. This choice of r_c particularly implies that in the perfect lattice, only heat conduction between closest neighbors are considered.

It is notable that for $i \in \partial\Omega$, its interaction with neighbors outside Ω also need to be taken into account. Therefore, we extend the computational model at both ends by two $\langle 111 \rangle$ planes, and determine the particle temperature therein by linear extrapolation along z-axis from inside Ω.

4 RESULTS AND DISCUSSION

As already mentioned, our objective in this computational study is not to predict, but rather to reproduce the size effect discovered in the experiment [8] based on the discrete kinetic potentials defined in Section 2. [8] have shown in their study (see Fig. 3(b) of [8]) that the temperature dependence of the thermal conductivity of Si nanowires at low

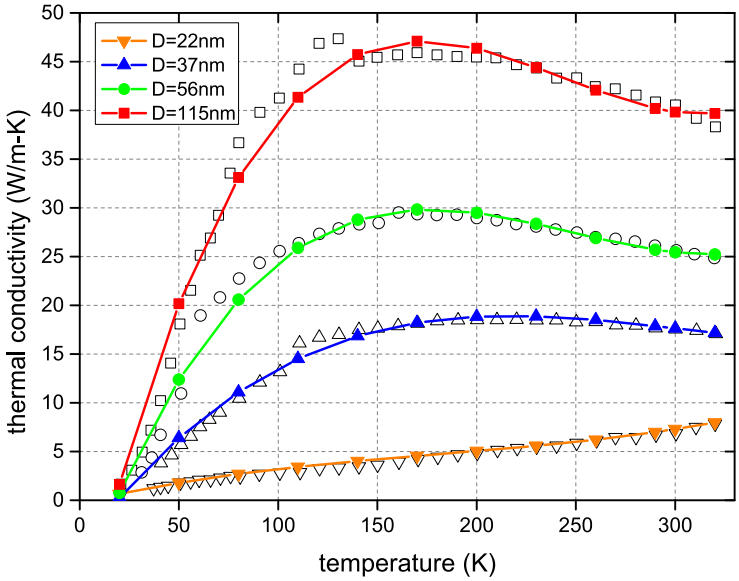

Figure 1: Comparison of numerical results (filled symbols) and experimental measurements (opened symbols [8]) for thermal conductivity in Si nanowires of different radii (the lines serve as a guide for the eye).

D	a_3	a_2	a_1	a_0
22 nm	$3.293 \cdot 10^{-7}$	$-1.422 \cdot 10^{-4}$	$6.993 \cdot 10^{-2}$	2.139
37 nm	$2.222 \cdot 10^{-6}$	$-1.829 \cdot 10^{-3}$	$4.753 \cdot 10^{-1}$	-10.078
56 nm	$3.672 \cdot 10^{-6}$	$-2.701 \cdot 10^{-3}$	$6.081 \cdot 10^{-1}$	-11.182
115 nm	$3.629 \cdot 10^{-6}$	$-2.595 \cdot 10^{-3}$	$5.660 \cdot 10^{-1}$	-11.763

Table 1: Coefficients a_i of the polynomial 19.

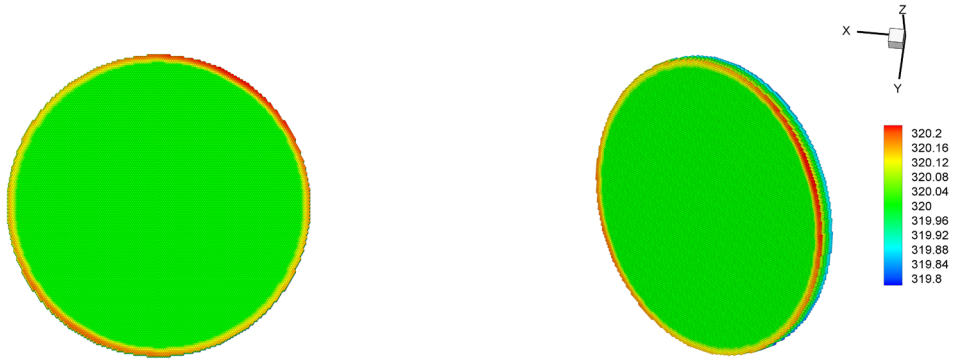

(a) (b)

Figure 2: Solution of particle temperature ($\{\theta\}$) for a nanowire slice with diameter $D = 56$ nm.

temperature follow a power law of exponents 3, 2 and 1, where the power exponent gets smaller as the diameter decreases. Thus, we postulate in this work that the variation of thermal conductivity in Si nanowires of different radii can be reproduced using the simplified discrete Fourier law [15] with

$$\begin{aligned} A_c(T) &= a_3 T^3 + a_2 T^2 + a_1 T + a_0 \\ A_a(T) &= 0.005 A_c(T) \end{aligned} \tag{19}$$

where a_i can be approximated by fitting our effective conductivity $\overline{\kappa}$ to the experimental measurements obtained by [8].

The effective conductivity $\overline{\kappa}$ obtained from each simulation is plotted in Fig. 1, in comparison with the experimental measurements extracted from Fig. 3(a) of [8]. The numerical results are in good agreement with the experimental data. In all simulations, we observe that θ is nearly uniform ($\sim T_0$) in the perfect crystal, but clearly varies in the amorphous surface layer. This is expected because the bondwise conductivity coefficient within the amorphous layer (A_a) is in all cases much smaller than that in the perfect crystalline core (A_c), one example is shown in Fig. 2.

5 SUMMARY

We have presented a validation case that illustrates the range and scope of our computational framework. This validation case is characterized by the need or desirability to account for atomic-level properties while simultaneously entailing tie scales much longer than those accessible to direct molecular dynamics.

ACKNOWLEDGEMENTS

CS.M. and MP.A. gratefully acknowledge the support of the Ministerio de Economía y Competitividad of Spain (DPI2012-32508). M.O. gratefully acknowledges support from the U. S. Army Research Laboratory (ARL) through the Materials in Extreme Dynamic Environments (MEDE) Collaborative Research Alliance (CRA) under Award Number W911NF-11-R-0001. CS.M. also acknowledges fellowship support from Ministerio de Economía y Competitividad of Spain (BES-2013-066591).

REFERENCES

[1] W. Kim, J. Zide, A. Gossard, D. Klenov, S. Stemmer, A. Shakouri, and A. Majumdar, "Thermal conductivity reduction and thermoelectric figure of merit increase by embedding nanoparticles in crystalline semiconductors," *Physical Review Letters*, vol. 96, no. 4, 2006.

[2] V. Shields, "Applications of silicon carbide for high temperature electronics and sensors," Tech Briefs 0145-319X, NASA Jet Propulsion Laboratory, 1995.

[3] T. C. Harman, P. J. Taylor, M. P. Walsh, and B. E. LaForge, "Quantum dot superlattice thermoelectric materials and devices," *Science*, vol. 297, no. 5590, pp. 2229–2232, 2002.

[4] W. Kim, "Thermal transport in individual thermoelectric nanowires: a review," *Materials Research Innovations*, vol. 15, no. 6, pp. 375–385, 2011.

[5] L. Hicks and M. Dresselhaus, "Thermoelectric figure of merit of a one-dimensional conductor," *Physical Review B*, vol. 47, no. 24, pp. 16631–16634, 1993.

[6] Y. Cui, L. Lauhon, M. Gudiksen, J. Wang, and C. Lieber, "Diameter-controlled synthesis of single-crystal silicon nanowires," *Applied Physics Letters*, vol. 78, no. 15, pp. 2214–2216, 2001.

[7] A. I. Hochbaum, R. Chen, R. D. Delgado, W. Liang, E. C. Garnett, M. Najarian, A. Majumdar, and P. Yang, "Enhanced thermoelectric performance of rough silicon nanowires," *Nature*, vol. 451, no. 7175, pp. 163–U5, 2008.

[8] D. Li, Y. Wu, P. Kim, L. Shi, P. Yang, and A. Majumdar, "Thermal conductivity of individual silicon nanowires," *Appl. Phys. Lett.*, vol. 83, no. 14, pp. 2934–2936, 2003.

[9] L. Shi, D. Li, C. Yu, W. Jang, D. Kim, Z. Yao, P. Kim, and A. Majumdar, "Measuring thermal and thermoelectric properties of one-dimensional nanostructures using a microfabricated device," *J. Heat Transfer*, vol. 125, pp. 881–888, 2003.

[10] R. Chen, A. I. Hochbaum, P. Murphy, J. Moore, P. Yang, and A. Majumdar, "Thermal conductance of thin silicon nanowires," *Physical Review Letters*, vol. 101, SEP 5 2008.

[11] G. S. Doerk, C. Carraro, and R. Maboudian, "Single Nanowire Thermal Conductivity Measurements by Raman Thermography," *ACS NANO*, vol. 4, no. 8, pp. 4908–4914, 2010.

[12] T. Markussen, A.-P. Jauho, and M. Brandbyge, "Heat conductance is strongly anisotropic for pristine silicon nanowires," *Nano Letters*, vol. 8, no. 11, pp. 3771–3775, 2008.

[13] D. Donadio and G. Galli, "Atomistic Simulations of Heat Transport in Silicon Nanowires," *Physical Review Letters*, vol. 102, no. 19, 2009.

[14] Y. Kulkarni, J. Knap, and M. Ortiz, "A Variational Approach to Coarse Graining of Equilibrium and Non-Equilibrium Atomistic Description at Finite Temperature," *J. Mech. Phys. Solids*, vol. 56, no. 4, pp. 1417–1449, 2008.

[15] G. Venturini, K. Wang, I. Romero, M. P. Ariza, and M. Ortiz, "Atomistic Long-Term Simulation of Heat and Mass Transport," *Journal of the Mechanics and Physics of Solids*, vol. (73), pp. 242–268, 2014.

[16] E. Blandre, L. Chaput, S. Merabia, D. Lacroix, and K. Termentzidis, "Modeling the reduction of thermal conductivity in core/shell and diameter-modulated silicon nanowires," *Physical Review B*, vol. 91, MAR 3 2015.

[17] F. Ross, J. Tersoff, and M. Reuter, "Sawtooth faceting in silicon nanowires," *Physical Review Letters*, vol. 95, SEP 30 2005.